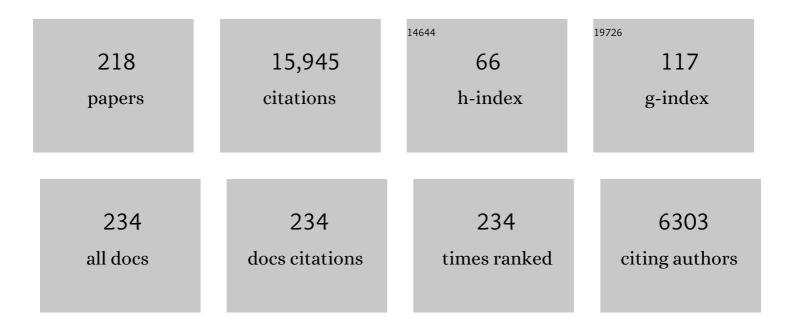
## Roger C Wiens

List of Publications by Year in descending order

Source: https://exaly.com/author-pdf/4028253/publications.pdf Version: 2024-02-01



#	Article	IF	CITATIONS
1	The SuperCam infrared spectrometer for the perseverance rover of the Mars2020 mission. Icarus, 2022, 373, 114773.	1.1	19
2	SuperCam calibration targets on board the perseverance rover: Fabrication and quantitative characterization. Spectrochimica Acta, Part B: Atomic Spectroscopy, 2022, 188, 106341.	1.5	20
3	Post-landing major element quantification using SuperCam laser induced breakdown spectroscopy. Spectrochimica Acta, Part B: Atomic Spectroscopy, 2022, 188, 106347.	1.5	40
4	Bedrock Geochemistry and Alteration History of the Clayâ€Bearing Glen Torridon Region of Gale Crater, Mars. Journal of Geophysical Research E: Planets, 2022, 127, .	1.5	17
5	An Insight Into Ancient Aeolian Processes and Postâ€Noachian Aqueous Alteration in Gale Crater, Mars, Using ChemCam Geochemical Data From the Greenheugh Capping Unit. Journal of Geophysical Research E: Planets, 2022, 127, .	1.5	11
6	In situ recording of Mars soundscape. Nature, 2022, 605, 653-658.	13.7	30
7	Optical calibration of the SuperCam instrument body unit spectrometers. Applied Optics, 2022, 61, 2967.	0.9	4
8	Overview of the Morphology and Chemistry of Diagenetic Features in the Clayâ€Rich Glen Torridon Unit of Gale Crater, Mars. Journal of Geophysical Research E: Planets, 2022, 127, .	1.5	17
9	Identifying Shocked Feldspar on Mars Using Perseverance Spectroscopic Instruments: Implications for Geochronology Studies on Returned Samples. Earth, Moon and Planets, 2022, 126, .	0.3	4
10	Homogeneity assessment of the SuperCam calibration targets onboard rover perseverance. Analytica Chimica Acta, 2022, 1209, 339837.	2.6	9
11	The dynamic atmospheric and aeolian environment of Jezero crater, Mars. Science Advances, 2022, 8, .	4.7	47
12	From Lake to River: Documenting an Environmental Transition Across the Jura/Knockfarril Hill Members Boundary in the Glen Torridon Region of Gale Crater (Mars). Journal of Geophysical Research E: Planets, 2022, 127, .	1.5	19
13	Barometric Pumping Through Fractured Rock: A Mechanism for Venting Deep Methane to Mars' Atmosphere. Geophysical Research Letters, 2022, 49, .	1.5	3
14	Deposition and erosion of a Light-Toned Yardang-forming unit of Mt Sharp, Gale crater, Mars. Earth and Planetary Science Letters, 2021, 554, 116681.	1.8	13
15	Experimental Wind Characterization with the SuperCam Microphone under a Simulated martian Atmosphere. Icarus, 2021, 354, 114060.	1.1	12
16	OrganiCam: a lightweight time-resolved laser-induced luminescence imager and Raman spectrometer for planetary organic material characterization. Applied Optics, 2021, 60, 3753.	0.9	3
17	The SuperCam Instrument Suite on the Mars 2020 Rover: Science Objectives and Mast-Unit Description. Space Science Reviews, 2021, 217, 1.	3.7	131
18	Alternating wet and dry depositional environments recorded in the stratigraphy of Mount Sharp at Gale crater, Mars. Geology, 2021, 49, 842-846.	2.0	33

#	Article	IF	CITATIONS
19	Perseverance's Scanning Habitable Environments with Raman and Luminescence for Organics and Chemicals (SHERLOC) Investigation. Space Science Reviews, 2021, 217, 1.	3.7	94
20	Quantification of manganese for ChemCam Mars and laboratory spectra using a multivariate model. Spectrochimica Acta, Part B: Atomic Spectroscopy, 2021, 181, 106223.	1.5	16
21	Brine-driven destruction of clay minerals in Gale crater, Mars. Science, 2021, 373, 198-204.	6.0	52
22	Improving ChemCam LIBS long-distance elemental compositions using empirical abundance trends. Spectrochimica Acta, Part B: Atomic Spectroscopy, 2021, 182, 106247.	1.5	16
23	Laser-Induced Breakdown Spectroscopy (LIBS) characterization of granular soils: Implications for ChemCam analyses at Gale crater, Mars. Icarus, 2021, 365, 114481.	1.1	11
24	The Genesis Solar-Wind Mission: first deep-space robotic mission to return to earth. , 2021, , 105-122.		2
25	The SuperCam Instrument Suite on the NASA Mars 2020 Rover: Body Unit and Combined System Tests. Space Science Reviews, 2021, 217, 4.	3.7	160
26	Perseverance rover reveals an ancient delta-lake system and flood deposits at Jezero crater, Mars. Science, 2021, 374, 711-717.	6.0	86
27	Clustering Supported Classification of ChemCam Data From Gale Crater, Mars. Earth and Space Science, 2021, 8, .	1.1	7
28	Long-Distance 3D Reconstructions Using Photogrammetry with Curiosity's ChemCam Remote Micro-Imager in Gale Crater (Mars). Remote Sensing, 2021, 13, 4068.	1.8	5
29	Acoustic monitoring of laser-induced phase transitions in minerals: implication for Mars exploration with SuperCam. Scientific Reports, 2021, 11, 24019.	1.6	12
30	Extraformational sediment recycling on Mars. , 2020, 16, 1508-1537.		20
31	Automatic preprocessing of laser-induced breakdown spectra using partial least squares regression and feed-forward artificial neural network: Applications to Earth and Mars data. Spectrochimica Acta, Part B: Atomic Spectroscopy, 2020, 171, 105930.	1.5	22
32	Mars 2020 Mission Overview. Space Science Reviews, 2020, 216, 1.	3.7	239
33	Analyses of Highâ€Iron Sedimentary Bedrock and Diagenetic Features Observed With ChemCam at Vera Rubin Ridge, Gale Crater, Mars: Calibration and Characterization. Journal of Geophysical Research E: Planets, 2020, 125, e2019JE006314.	1.5	30
34	Evidence for a Diagenetic Origin of Vera Rubin Ridge, Gale Crater, Mars: Summary and Synthesis of <i>Curiosity</i> 's Exploration Campaign. Journal of Geophysical Research E: Planets, 2020, 125, e2020JE006527.	1.5	69
35	Pre-launch radiometric calibration of the infrared spectrometer onboard SuperCam for the Mars2020 rover. Review of Scientific Instruments, 2020, 91, 063105.	0.6	10
36	Synergistic Ground and Orbital Observations of Iron Oxides on Mt. Sharp and Vera Rubin Ridge. Journal of Geophysical Research E: Planets, 2020, 125, e2019JE006294.	1.5	27

#	Article	IF	CITATIONS
37	Recording laser-induced sparks on Mars with the SuperCam microphone. Spectrochimica Acta, Part B: Atomic Spectroscopy, 2020, 174, 106000.	1.5	25
38	Spectral, Compositional, and Physical Properties of the Upper Murray Formation and Vera Rubin Ridge, Gale Crater, Mars. Journal of Geophysical Research E: Planets, 2020, 125, e2019JE006290.	1.5	20
39	Iron Mobility During Diagenesis at Vera Rubin Ridge, Gale Crater, Mars. Journal of Geophysical Research E: Planets, 2020, 125, e2019JE006299.	1.5	30
40	Boron and Lithium in Calcium Sulfate Veins: Tracking Precipitation of Diagenetic Materials in Vera Rubin Ridge, Gale Crater. Journal of Geophysical Research E: Planets, 2020, 125, e2019JE006301.	1.5	8
41	SuperCam Calibration Targets: Design and Development. Space Science Reviews, 2020, 216, 138.	3.7	44
42	Mars Extant Life: What's Next? Conference Report. Astrobiology, 2020, 20, 785-814.	1.5	56
43	Laser-induced breakdown spectroscopy in planetary science. , 2020, , 441-471.		4
44	Origin and composition of three heterolithic boulder- and cobble-bearing deposits overlying the Murray and Stimson formations, Gale Crater, Mars. Icarus, 2020, 350, 113897.	1.1	11
45	The Chemostratigraphy of the Murray Formation and Role of Diagenesis at Vera Rubin Ridge in Gale Crater, Mars, as Observed by the ChemCam Instrument. Journal of Geophysical Research E: Planets, 2020, 125, e2019JE006320.	1.5	41
46	Studies of a Lacustrineâ€Volcanic Mars Analog Field Site With Marsâ€2020â€Like Instruments. Earth and Space Science, 2020, 7, e2019EA000720.	1.1	18
47	Magnesium isotopes of the bulk solar wind from Genesis diamondâ€like carbon films. Meteoritics and Planetary Science, 2020, 55, 352-375.	0.7	12
48	Grain Size Variations in the Murray Formation: Stratigraphic Evidence for Changing Depositional Environments in Gale Crater, Mars. Journal of Geophysical Research E: Planets, 2020, 125, e2019JE006230.	1.5	29
49	Geochemical variation in the Stimson formation of Gale crater: Provenance, mineral sorting, and a comparison with modern Martian dunes. Icarus, 2020, 341, 113622.	1.1	31
50	Mineralogy and geochemistry of sedimentary rocks and eolian sediments in Gale crater, Mars: A review after six Earth years of exploration with Curiosity. Chemie Der Erde, 2020, 80, 125605.	0.8	137
51	Identification and Description of a Silicic Volcaniclastic Layer in Gale Crater, Mars, Using Active Neutron Interrogation. Journal of Geophysical Research E: Planets, 2020, 125, e2019JE006180.	1.5	16
52	Hydrogen Variability in the Murray Formation, Gale Crater, Mars. Journal of Geophysical Research E: Planets, 2020, 125, e2019JE006289.	1.5	12
53	Pulsed laser-induced heating of mineral phases: Implications for laser-induced breakdown spectroscopy combined with Raman spectroscopy. Spectrochimica Acta, Part B: Atomic Spectroscopy, 2019, 160, 105687.	1.5	27
54	Mars Science Laboratory Observations of Chloride Salts in Gale Crater, Mars. Geophysical Research Letters, 2019, 46, 10754-10763.	1.5	52

#	Article	IF	CITATIONS
55	An interval of high salinity in ancient Gale crater lake on Mars. Nature Geoscience, 2019, 12, 889-895.	5.4	105
56	Mineralâ€Filled Fractures as Indicators of Multigenerational Fluid Flow in the Pahrump Hills Member of the Murray Formation, Gale Crater, Mars. Earth and Space Science, 2019, 6, 238-265.	1.1	66
57	Listening to laser sparks: a link between Laser-Induced Breakdown Spectroscopy, acoustic measurements and crater morphology. Spectrochimica Acta, Part B: Atomic Spectroscopy, 2019, 153, 50-60.	1.5	57
58	Elemental Analyses of Mars from Rovers with Laser-Induced Breakdown Spectroscopy by ChemCam and SuperCam. , 2019, , 573-587.		0
59	Late-stage diagenetic concretions in the Murray formation, Gale crater, Mars. Icarus, 2019, 321, 866-890.	1.1	50
60	Copper enrichments in the Kimberley formation in Gale crater, Mars: Evidence for a Cu deposit at the source. Icarus, 2019, 321, 736-751.	1.1	23
61	Chemical alteration of fine-grained sedimentary rocks at Gale crater. Icarus, 2019, 321, 619-631.	1.1	52
62	Alteration trends and geochemical source region characteristics preserved in the fluviolacustrine sedimentary record of Gale crater, Mars. Geochimica Et Cosmochimica Acta, 2019, 246, 234-266.	1.6	39
63	Using ChemCam LIBS data to constrain grain size in rocks on Mars: Proof of concept and application to rocks at Yellowknife Bay and Pahrump Hills, Gale crater. Icarus, 2019, 321, 82-98.	1.1	37
64	Laser-induced breakdown spectroscopy acoustic testing of the Mars 2020 microphone. Planetary and Space Science, 2019, 165, 260-271.	0.9	32
65	Investigating the role of anhydrous oxidative weathering on sedimentary rocks in the Transantarctic Mountains and implications for the modern weathering of sedimentary lithologies on Mars. Icarus, 2019, 319, 669-684.	1.1	8
66	The SuperCam infrared instrument on the NASA MARS2020 mission: performance and qualification results. , 2019, , .		5
67	Retrieval of water vapor column abundance and aerosol properties from ChemCam passive sky spectroscopy. Icarus, 2018, 307, 294-326.	1.1	39
68	Chemical variability in mineralized veins observed by ChemCam on the lower slopes of Mount Sharp in Gale crater, Mars. Icarus, 2018, 311, 69-86.	1.1	34
69	Shaler: <i>inÂsitu</i> analysis of a fluvial sedimentary deposit on Mars. Sedimentology, 2018, 65, 96-122.	1.6	59
70	Gypsum, bassanite, and anhydrite at Gale crater, Mars. American Mineralogist, 2018, 103, 1011-1020.	0.9	96
71	Desiccation cracks provide evidence of lake drying on Mars, Sutton Island member, Murray formation, Gale Crater. Geology, 2018, 46, 515-518.	2.0	71
72	Martian Eolian Dust Probed by ChemCam. Geophysical Research Letters, 2018, 45, 10,968.	1.5	40

#	Article	IF	CITATIONS
73	In Situ Analysis of Opal in Gale Crater, Mars. Journal of Geophysical Research E: Planets, 2018, 123, 1955-1972.	1.5	36
74	Bagnold Dunes Campaign Phase 2: Visible/Nearâ€Infrared Reflectance Spectroscopy of Longitudinal Ripple Sands. Geophysical Research Letters, 2018, 45, 9480-9487.	1.5	17
75	The NASA Mars 2020 Rover Mission and the Search for Extraterrestrial Life. , 2018, , 275-308.		95
76	Incorporating AEGIS autonomous science into Mars Science Laboratory rover mission operations. , 2018, , .		2
77	Characterization of Hydrogen in Basaltic Materials With Laserâ€Induced Breakdown Spectroscopy ( <scp>LIBS</scp> ) for Application to <scp>MSL</scp> ChemCam Data. Journal of Geophysical Research E: Planets, 2018, 123, 1996-2021.	1.5	32
78	Simulated laser-induced breakdown spectra of graphite and synthetic shergottite glass under Martian conditions. Spectrochimica Acta, Part B: Atomic Spectroscopy, 2018, 148, 31-43.	1.5	7
79	Spark plasma sintering preparation of reference targets for field spectroscopy on Mars. Journal of Raman Spectroscopy, 2018, 49, 1419-1425.	1.2	11
80	Recalibration of the Mars Science Laboratory ChemCam instrument with an expanded geochemical database. Spectrochimica Acta, Part B: Atomic Spectroscopy, 2017, 129, 64-85.	1.5	137
81	Quantification of water content by laser induced breakdown spectroscopy on Mars. Spectrochimica Acta, Part B: Atomic Spectroscopy, 2017, 130, 82-100.	1.5	65
82	Classification of igneous rocks analyzed by ChemCam at Gale crater, Mars. Icarus, 2017, 288, 265-283.	1.1	96
83	Visible/nearâ€infrared spectral diversity from in situ observations of the Bagnold Dune Field sands in Gale Crater, Mars. Journal of Geophysical Research E: Planets, 2017, 122, 2655-2684.	1.5	40
84	AEGIS autonomous targeting for ChemCam on Mars Science Laboratory: Deployment and results of initial science team use. Science Robotics, 2017, 2, .	9.9	76
85	Diagenetic silica enrichment and lateâ€stage groundwater activity in Gale crater, Mars. Geophysical Research Letters, 2017, 44, 4716-4724.	1.5	87
86	Redox stratification of an ancient lake in Gale crater, Mars. Science, 2017, 356, .	6.0	209
87	Chemistry, mineralogy, and grain properties at Namib and High dunes, Bagnold dune field, Gale crater, Mars: A synthesis of Curiosity rover observations. Journal of Geophysical Research E: Planets, 2017, 122, 2510-2543.	1.5	95
88	Centimeter to decimeter hollow concretions and voids in Gale Crater sediments, Mars. Icarus, 2017, 289, 144-156.	1.1	12
89	Alkali trace elements in Gale crater, Mars, with ChemCam: Calibration update and geological implications. Journal of Geophysical Research E: Planets, 2017, 122, 650-679.	1.5	48
90	Characterization of LIBS emission lines for the identification of chlorides, carbonates, and sulfates in salt/basalt mixtures for the application to MSL ChemCam data. Journal of Geophysical Research E: Planets, 2017, 122, 744-770.	1.5	57

#	Article	IF	CITATIONS
91	Improved accuracy in quantitative laser-induced breakdown spectroscopy using sub-models. Spectrochimica Acta, Part B: Atomic Spectroscopy, 2017, 129, 49-57.	1.5	71
92	Geologic overview of the Mars Science Laboratory rover mission at the Kimberley, Gale crater, Mars. Journal of Geophysical Research E: Planets, 2017, 122, 2-20.	1.5	60
93	Roughness effects on the hydrogen signal in laser-induced breakdown spectroscopy. Spectrochimica Acta, Part B: Atomic Spectroscopy, 2017, 137, 13-22.	1.5	34
94	In situ detection of boron by ChemCam on Mars. Geophysical Research Letters, 2017, 44, 8739-8748.	1.5	56
95	Understanding heterogeneity in Genesis diamond-like carbon film using SIMS analysis of implants. Journal of Materials Science, 2017, 52, 11282-11305.	1.7	7
96	Branching Ratios in Vacuum Ultraviolet Photodissociation of CO and N <sub>2</sub> : Implications for Oxygen and Nitrogen Isotopic Compositions of the Solar Nebula. Astrophysical Journal, 2017, 850, 48.	1.6	17
97	Basalt–trachybasalt samples in Gale Crater, Mars. Meteoritics and Planetary Science, 2017, 52, 2931-2410.	0.7	34
98	Geochemistry of the Bagnold dune field as observed by ChemCam and comparison with other aeolian deposits at Gale Crater. Journal of Geophysical Research E: Planets, 2017, 122, 2144-2162.	1.5	46
99	Classification scheme for sedimentary and igneous rocks in Gale crater, Mars. Icarus, 2017, 284, 1-17.	1.1	46
100	Fluidized-sediment pipes in Gale crater, Mars, and possible Earth analogs. Geology, 2017, 45, 7-10.	2.0	18
101	Chemistry of diagenetic features analyzed by ChemCam at Pahrump Hills, Gale crater, Mars. Icarus, 2017, 281, 121-136.	1.1	90
102	Determining the Elemental and Isotopic Composition of the Pre-solar Nebula from Genesis Data Analysis: The Case of Oxygen. Astrophysical Journal Letters, 2017, 851, L12.	3.0	15
103	The supercam infrared instrument on the NASA Mars2020 mission: optical design and performance. , 2017, , .		3
104	Constraints on iron sulfate and iron oxide mineralogy from ChemCam visible/near-infrared reflectance spectroscopy of Mt. Sharp basal units, Gale Crater, Mars. American Mineralogist, 2016, 101, 1501-1514.	0.9	31
105	Oxidation of manganese in an ancient aquifer, Kimberley formation, Gale crater, Mars. Geophysical Research Letters, 2016, 43, 7398-7407.	1.5	110
106	Restoration of the Autofocus capability of the ChemCam instrument onboard the Curiosity rover. , 2016, , .		8
107	Observation of > 5 wt % zinc at the Kimberley outcrop, Gale crater, Mars. Journal of Geophysical Research E: Planets, 2016, 121, 338-352.	1.5	32
108	Composition of conglomerates analyzed by the Curiosity rover: Implications for Gale Crater crust and sediment sources. Journal of Geophysical Research E: Planets, 2016, 121, 353-387.	1.5	53

#	Article	IF	CITATIONS
109	Analysis of geological materials containing uranium using laser-induced breakdown spectroscopy. Spectrochimica Acta, Part B: Atomic Spectroscopy, 2016, 120, 1-8.	1.5	40
110	Application of distance correction to ChemCam laser-induced breakdown spectroscopy measurements. Spectrochimica Acta, Part B: Atomic Spectroscopy, 2016, 120, 19-29.	1.5	27
111	Magmatic complexity on early Mars as seen through a combination of orbital, in-situ and meteorite data. Lithos, 2016, 254-255, 36-52.	0.6	66
112	Mineralogy, provenance, and diagenesis of a potassic basaltic sandstone on Mars: CheMin Xâ€ray diffraction of the Windjana sample (Kimberley area, Gale Crater). Journal of Geophysical Research E: Planets, 2016, 121, 75-106.	1.5	159
113	Hydration state of calcium sulfates in Gale crater, Mars: Identification of bassanite veins. Earth and Planetary Science Letters, 2016, 452, 197-205.	1.8	103
114	Fluids during diagenesis and sulfate vein formation in sediments at Gale crater, Mars. Meteoritics and Planetary Science, 2016, 51, 2175-2202.	0.7	50
115	"Standoff Biofinder―for Fast, Noncontact, Nondestructive, Large-Area Detection of Biological Materials for Planetary Exploration. Astrobiology, 2016, 16, 715-729.	1.5	12
116	The potassic sedimentary rocks in Gale Crater, Mars, as seen by ChemCam on board <i>Curiosity</i> . Journal of Geophysical Research E: Planets, 2016, 121, 784-804.	1.5	67
117	ChemCam investigation of the John Klein and Cumberland drill holes and tailings, Gale crater, Mars. Icarus, 2016, 277, 330-341.	1.1	6
118	ChemCam activities and discoveries during the nominal mission of the Mars Science Laboratory in Gale crater, Mars. Journal of Analytical Atomic Spectrometry, 2016, 31, 863-889.	1.6	134
119	AEGIS autonomous targeting for the Curiosity rover's ChemCam instrument. , 2015, , .		13
120	Diagenesis and clay mineral formation at Gale Crater, Mars. Journal of Geophysical Research E: Planets, 2015, 120, 1-19.	1.5	72
121	VARIATIONS IN SOLAR WIND FRACTIONATION AS SEEN BY <i>ACE</i> /SWICS AND THE IMPLICATIONS FOR <i>GENESIS</i> MISSION RESULTS. Astrophysical Journal, 2015, 812, 1.	1.6	24
122	SHERLOC: Scanning habitable environments with Raman & luminescence for organics & chemicals. , 2015, , .		67
123	Chemical variations in Yellowknife Bay formation sedimentary rocks analyzed by ChemCam on board the Curiosity rover on Mars. Journal of Geophysical Research E: Planets, 2015, 120, 452-482.	1.5	51
124	Hydrogen detection with ChemCam at Gale crater. Icarus, 2015, 249, 43-61.	1.1	58
125	First detection of fluorine on Mars: Implications for Gale Crater's geochemistry. Geophysical Research Letters, 2015, 42, 1020-1028.	1.5	107
126	ChemCam: Chemostratigraphy by the First Mars Microprobe. Elements, 2015, 11, 33-38.	0.5	54

#	Article	IF	CITATIONS
127	Theoretical modeling and analysis of the emission spectra of a ChemCam standard: Basalt BIR-1A. Spectrochimica Acta, Part B: Atomic Spectroscopy, 2015, 110, 20-30.	1.5	8
128	In situ evidence for continental crust on early Mars. Nature Geoscience, 2015, 8, 605-609.	5.4	233
129	Evidence for indigenous nitrogen in sedimentary and aeolian deposits from the <i>Curiosity</i> rover investigations at Gale crater, Mars. Proceedings of the National Academy of Sciences of the United States of America, 2015, 112, 4245-4250.	3.3	172
130	Deposition, exhumation, and paleoclimate of an ancient lake deposit, Gale crater, Mars. Science, 2015, 350, aac7575.	6.0	471
131	Gale crater and impact processes – Curiosity's first 364 Sols on Mars. Icarus, 2015, 249, 108-128.	1.1	37
132	Compositions of coarse and fine particles in martian soils at gale: A window into the production of soils. Icarus, 2015, 249, 22-42.	1.1	64
133	The ChemCam Remote Micro-Imager at Gale crater: Review of the first year of operations on Mars. Icarus, 2015, 249, 93-107.	1.1	95
134	Understanding the signature of rock coatings in laser-induced breakdown spectroscopy data. Icarus, 2015, 249, 62-73.	1.1	49
135	ChemCam passive reflectance spectroscopy of surface materials at the Curiosity landing site, Mars. Icarus, 2015, 249, 74-92.	1.1	70
136	ChemCam results from the Shaler outcrop in Gale crater, Mars. Icarus, 2015, 249, 2-21.	1.1	52
137	Two Years of Operations of the ChemCam Instrument Onboard the Curiosity Rover. , 2015, , 403-434.		Ο
138	High manganese concentrations in rocks at Gale crater, Mars. Geophysical Research Letters, 2014, 41, 5755-5763.	1.5	81
139	Trace element geochemistry (Li, Ba, Sr, and Rb) using <i>Curiosity</i> 's ChemCam: Early results for Gale crater from Bradbury Landing Site to Rocknest. Journal of Geophysical Research E: Planets, 2014, 119, 255-285.	1.5	86
140	Correcting for variable laser-target distances of laser-induced breakdown spectroscopy measurements with ChemCam using emission lines of Martian dust spectra. Spectrochimica Acta, Part B: Atomic Spectroscopy, 2014, 96, 51-60.	1.5	45
141	Volatile and Organic Compositions of Sedimentary Rocks in Yellowknife Bay, Gale Crater, Mars. Science, 2014, 343, 1245267.	6.0	323
142	A Habitable Fluvio-Lacustrine Environment at Yellowknife Bay, Gale Crater, Mars. Science, 2014, 343, 1242777.	6.0	687
143	Elemental Geochemistry of Sedimentary Rocks at Yellowknife Bay, Gale Crater, Mars. Science, 2014, 343, 1244734.	6.0	246
144	Calcium sulfate veins characterized by ChemCam/Curiosity at Gale crater, Mars. Journal of Geophysical Research E: Planets, 2014, 119, 1991-2016.	1.5	214

#	Article	IF	CITATIONS
145	In situ calibration using univariate analyses based on the onboard ChemCam targets: first prediction of Martian rock and soil compositions. Spectrochimica Acta, Part B: Atomic Spectroscopy, 2014, 99, 34-51.	1.5	45
146	Terrain physical properties derived from orbital data and the first 360 sols of Mars Science Laboratory Curiosity rover observations in Gale Crater. Journal of Geophysical Research E: Planets, 2014, 119, 1322-1344.	1.5	43
147	The rock abrasion record at Gale Crater: Mars Science Laboratory results from Bradbury Landing to Rocknest. Journal of Geophysical Research E: Planets, 2014, 119, 1374-1389.	1.5	46
148	Diagenetic origin of nodules in the Sheepbed member, Yellowknife Bay formation, Gale crater, Mars. Journal of Geophysical Research E: Planets, 2014, 119, 1637-1664.	1.5	80
149	Overview of the Mars Science Laboratory mission: Bradbury Landing to Yellowknife Bay and beyond. Journal of Geophysical Research E: Planets, 2014, 119, 1134-1161.	1.5	104
150	Geochemical diversity in first rocks examined by the Curiosity Rover in Gale Crater: Evidence for and significance of an alkali and volatileâ€rich igneous source. Journal of Geophysical Research E: Planets, 2014, 119, 64-81.	1.5	113
151	Chemistry and texture of the rocks at Rocknest, Gale Crater: Evidence for sedimentary origin and diagenetic alteration. Journal of Geophysical Research E: Planets, 2014, 119, 2109-2131.	1.5	48
152	Chemistry of fractureâ€filling raised ridges in Yellowknife Bay, Gale Crater: Window into past aqueous activity and habitability on Mars. Journal of Geophysical Research E: Planets, 2014, 119, 2398-2415.	1.5	70
153	Igneous mineralogy at Bradbury Rise: The first ChemCam campaign at Gale crater. Journal of Geophysical Research E: Planets, 2014, 119, 30-46.	1.5	114
154	Planetary Geochemical Investigations Using Raman and Laser-Induced Breakdown Spectroscopy. Applied Spectroscopy, 2014, 68, 925-936.	1.2	56
155	The Genesis Solar Wind Concentrator: Flight and Post-Flight Conditions and Modeling of Instrumental Fractionation. Space Science Reviews, 2013, 175, 93-124.	3.7	6
156	Solar Wind Conditions and Composition During the Genesis Mission as Measured by in situ Spacecraft. Space Science Reviews, 2013, 175, 125-164.	3.7	36
157	Pre-flight calibration and initial data processing for the ChemCam laser-induced breakdown spectroscopy instrument on the Mars Science Laboratory rover. Spectrochimica Acta, Part B: Atomic Spectroscopy, 2013, 82, 1-27.	1.5	258
158	Independent component analysis classification of laser induced breakdown spectroscopy spectra. Spectrochimica Acta, Part B: Atomic Spectroscopy, 2013, 86, 31-41.	1.5	66
159	Abundance and Isotopic Composition of Gases in the Martian Atmosphere from the Curiosity Rover. Science, 2013, 341, 263-266.	6.0	327
160	Volatile, Isotope, and Organic Analysis of Martian Fines with the Mars Curiosity Rover. Science, 2013, 341, 1238937.	6.0	367
161	Martian Fluvial Conglomerates at Gale Crater. Science, 2013, 340, 1068-1072.	6.0	326
162	The Petrochemistry of Jake_M: A Martian Mugearite. Science, 2013, 341, 1239463.	6.0	134

#	Article	IF	CITATIONS
163	Soil Diversity and Hydration as Observed by ChemCam at Gale Crater, Mars. Science, 2013, 341, 1238670.	6.0	215
164	Characteristics of pebble―and cobbleâ€sized clasts along the Curiosity rover traverse from Bradbury Landing to Rocknest. Journal of Geophysical Research E: Planets, 2013, 118, 2361-2380.	1.5	44
165	Solar Wind Concentrator. Geophysical Monograph Series, 2013, , 195-200.	0.1	3
166	Examining natural rock varnish and weathering rinds with laser-induced breakdown spectroscopy for application to ChemCam on Mars. Applied Optics, 2012, 51, B74.	0.9	49
167	Comparison of two partial least squares-discriminant analysis algorithms for identifying geological samples with the ChemCam laser-induced breakdown spectroscopy instrument. Applied Optics, 2012, 51, B130.	0.9	33
168	ISOTOPIC MASS FRACTIONATION OF SOLAR WIND: EVIDENCE FROM FAST AND SLOW SOLAR WIND COLLECTED BY THE <i>GENESIS</i> MISSION. Astrophysical Journal, 2012, 759, 121.	1.6	75
169	Remote laserâ€induced breakdown spectroscopy (LIBS) for lunar exploration. Journal of Geophysical Research, 2012, 117, .	3.3	55
170	Ceramic ChemCam Calibration Targets on Mars Science Laboratory. Space Science Reviews, 2012, 170, 229-255.	3.7	52
171	Mars Science Laboratory Mission and Science Investigation. Space Science Reviews, 2012, 170, 5-56.	3.7	650
172	The ChemCam Instrument Suite on the Mars Science Laboratory (MSL) Rover: Body Unit and Combined System Tests. Space Science Reviews, 2012, 170, 167-227.	3.7	429
173	The ChemCam Instrument Suite on the Mars Science Laboratory (MSL) Rover: Science Objectives and Mast Unit Description. Space Science Reviews, 2012, 170, 95-166.	3.7	372
174	Gale Crater: Formation and post-impact hydrous environments. Planetary and Space Science, 2012, 70, 84-95.	0.9	67
175	Clustering and training set selection methods for improving the accuracy of quantitative laser induced breakdown spectroscopy. Spectrochimica Acta, Part B: Atomic Spectroscopy, 2012, 70, 24-32.	1.5	41
176	Puncturing Mars: How impact craters interact with the Martian cryosphere. Earth and Planetary Science Letters, 2012, 335-336, 9-17.	1.8	46
177	Textural and modal analyses of picritic basalts with ChemCam Laserâ€Induced Breakdown Spectroscopy. Journal of Geophysical Research, 2012, 117, .	3.3	23
178	Mars Science Laboratory Mission and Science Investigation. , 2012, , 5-56.		23
179	The ChemCam Instrument Suite on the Mars Science Laboratory (MSL) Rover: Body Unit and Combined System Tests. , 2012, , 167-227.		6
180	The Oxygen Isotopic Composition of the Sun Inferred from Captured Solar Wind. Science, 2011, 332, 1528-1532.	6.0	321

#	Article	IF	CITATIONS
181	Isotopic and elemental fractionation of solar wind implanted in the Genesis concentrator target characterized and quantified by noble gases. Meteoritics and Planetary Science, 2011, 46, 493-512.	0.7	13
182	Laser induced breakdown spectroscopy library for the Martian environment. Spectrochimica Acta, Part B: Atomic Spectroscopy, 2011, 66, 805-814.	1.5	86
183	The influence of multivariate analysis methods and target grain size on the accuracy of remote quantitative chemical analysis of rocks using laser induced breakdown spectroscopy. Icarus, 2011, 215, 608-627.	1.1	81
184	Nonlinear mapping technique for data visualization and clustering assessment of LIBS data: application to ChemCam data. Analytical and Bioanalytical Chemistry, 2011, 400, 3247-3260.	1.9	40
185	Onboard calibration igneous targets for the Mars Science Laboratory Curiosity rover and the Chemistry Camera laser induced breakdown spectroscopy instrument. Spectrochimica Acta, Part B: Atomic Spectroscopy, 2011, 66, 280-289.	1.5	90
186	Strategies for Mars remote Laser-Induced Breakdown Spectroscopy analysis of sulfur in geological samples. Spectrochimica Acta, Part B: Atomic Spectroscopy, 2011, 66, 39-56.	1.5	107
187	A <sup>15</sup> N-Poor Isotopic Composition for the Solar System As Shown by Genesis Solar Wind Samples. Science, 2011, 332, 1533-1536.	6.0	255
188	Calibrating the ChemCam laser-induced breakdown spectroscopy instrument for carbonate minerals on Mars. Applied Optics, 2010, 49, C211.	2.1	81
189	Nitrogen isotopes in the recent solar wind from the analysis of Genesis targets: Evidence for large scale isotope heterogeneity in the early solar system. Geochimica Et Cosmochimica Acta, 2010, 74, 340-355.	1.6	94
190	Optimization of laser-induced breakdown spectroscopy for rapid geochemical analysis. Chemical Geology, 2010, 277, 137-148.	1.4	104
191	Multivariate analysis of remote laser-induced breakdown spectroscopy spectra using partial least squares, principal component analysis, and related techniques. Spectrochimica Acta, Part B: Atomic Spectroscopy, 2009, 64, 79-88.	1.5	266
192	Combined remote LIBS and Raman spectroscopy at 8.6m of sulfur-containing minerals, and minerals coated with hematite or covered with basaltic dust. Spectrochimica Acta - Part A: Molecular and Biomolecular Spectroscopy, 2007, 68, 1036-1045.	2.0	111
193	The Genesis Solar Wind Concentrator Target: Mass Fractionation Characterised by Neon Isotopes. Space Science Reviews, 2007, 130, 309-316.	3.7	11
194	Elemental Abundances of the Bulk Solar Wind: Analyses from Genesis and ACE. Space Science Reviews, 2007, 130, 79-86.	3.7	50
195	Solar and Solar-Wind Composition Results fromÂtheÂGenesis Mission. Space Science Reviews, 2007, 130, 161-171.	3.7	10
196	Solar and Solar-Wind Composition Results fromÂtheÂGenesis Mission. Space Sciences Series of ISSI, 2007, , 161-171.	0.0	1
197	The Genesis Solar Wind Concentrator Target: Mass Fractionation Characterised by Neon Isotopes. Space Sciences Series of ISSI, 2007, , 309-316.	0.0	2
198	Remote laser-induced breakdown spectroscopy analyses of Dar al Gani 476 and Zagami Martian meteorites. Journal of Geophysical Research, 2006, 111, .	3.3	50

#	Article	IF	CITATIONS
199	Joint analyses by laser-induced breakdown spectroscopy (LIBS) and Raman spectroscopy at stand-off distances. Spectrochimica Acta - Part A: Molecular and Biomolecular Spectroscopy, 2005, 61, 2324-2334.	2.0	128
200	Evaluation of a compact spectrograph for in-situ and stand-off Laser-Induced Breakdown Spectroscopy analyses of geological samples on Mars missions. Spectrochimica Acta, Part B: Atomic Spectroscopy, 2005, 60, 805-815.	1.5	121
201	Laser-Induced Breakdown Spectroscopy for Mars surface analysis: capabilities at stand-off distances and detection of chlorine and sulfur elements. Spectrochimica Acta, Part B: Atomic Spectroscopy, 2004, 59, 1413-1422.	1.5	163
202	Solar and solar-wind isotopic compositions. Earth and Planetary Science Letters, 2004, 222, 697-712.	1.8	46
203	Erratum to "Solar and solar-wind isotopic compositions―[Earth Planet. Sci. Lett. 224 (2004) 697–712]. Earth and Planetary Science Letters, 2004, 226, 547.	1.8	1
204	Analysis of Water Ice and Water Ice/Soil Mixtures Using Laser-Induced Breakdown Spectroscopy: Application to Mars Polar Exploration. Applied Spectroscopy, 2004, 58, 897-909.	1.2	62
205	The Genesis Solar Wind Concentrator. Space Science Reviews, 2003, 105, 561-599.	3.7	17
206	The Genesis Discovery Mission: Return of Solar Matter to Earth. Space Science Reviews, 2003, 105, 509-534.	3.7	108
207	The Plasma Ion and Electron Instruments for the Genesis Mission. Space Science Reviews, 2003, 105, 627-660.	3.7	25
208	The Genesis Solar-Wind Collector Materials. Space Science Reviews, 2003, 105, 535-560.	3.7	57
209	Genesis Solar Wind Concentrator: Computer Simulations of Performance Under Solar Wind Conditions. Space Science Reviews, 2003, 105, 601-626.	3.7	21
210	Genesis on-board determination of the solar wind flow regime. Space Science Reviews, 2003, 105, 661-679.	3.7	56
211	Genesis Solar Wind Concentrator: Computer Simulations of Performance under Solar Wind Conditions. , 2003, , 93-117.		5
212	The Genesis Discovery Mission: Return of Solar Matter to Earth. , 2003, , 1-26.		20
213	The Genesis Solar Wind Concentrator. , 2003, , 53-91.		4
214	Genesis mission to return solar winds samples to Earth. Eos, 2002, 83, 229.	0.1	2
215	Combined remote mineralogical and elemental identification from rovers: Field and laboratory tests using reflectance and laser-induced breakdown spectroscopy. Journal of Geophysical Research, 2002, 107, FIDO 3-1-FIDO 3-14.	3.3	54
216	The solar oxygenâ€isotopic composition: Predictions and implications for solar nebula processes. Meteoritics and Planetary Science, 1999, 34, 99-107.	0.7	52

#	Article	IF	CITATIONS
217	Laboratory shock emplacement of noble gases, nitrogen, and carbon dioxide into basalt, and implications for trapped gases in shergottite EETA 79001. Geochimica Et Cosmochimica Acta, 1988, 52, 295-307.	1.6	89
218	The case for a martian origin of the shergottites, II. Trapped and indigenous gas components in EETA 79001 glass. Earth and Planetary Science Letters, 1986, 77, 149-158.	1.8	108